ES Mater. Manuf., 2024, **24**,1165

ES Materials and Manufacturing
DOI: https://dx.doi.org/10.30919/esmm1165

Study of the Effect of Nanostructured Grains on the Radiation Resistance of Zirconium Dioxide Ceramics During Gas Swelling in the Case of High-Dose Irradiation with He^{2+} Ions

Artem L. Kozlovskiy,[1, 2,*] Marina Konuhova,[3] Dmitriy I. Shlimas,[1, 2] Daryn B. Borgekov,[1, 2] Maxim V. Zdorovets,[1, 2] Rafael I. Shakirziyanov,[1] Yuriy A. Garanin,[1] Natalia O. Volodina[1] and Anatoli I. Popov[3]

Abstract

The paper is devoted to the study of the influence of variation of ZrO_2 ceramics grain sizes on the resistance to radiation-induced swelling under irradiation with low-energy He^{2+} ions. The choice of ZrO_2 ceramics as objects of research is due to high levels of mechanical strength and hardness, as well as low rates of thermal expansion, which eliminates the effects of thermal expansion and destruction when operating at high temperatures, as well as good insulating properties, which makes it possible to use these ceramics both as radiation-resistant materials in nuclear energy in the manufacture of inert matrices of dispersed nuclear fuel, and as a basis for creation of fuel cells for the production of hydrogen. During the studies of the influence of mechanochemical grinding conditions on the change in dimensional factors in ZrO_2 ceramics, it was found that increasing the grinding speed from 300 to 900 rpm does not lead to the initiation of polymorphic transformation processes of the m-ZrO_2 → t-ZrO_2 type, which are also not initiated during thermal annealing of samples at a temperature of 1500 °C, the choice of which was due to thermal relaxation of structural deformation distortions caused by mechanochemical grinding during grain crushing. In determining the influence of size effects (dislocation strengthening) on the resistance of ZrO_2 ceramics to radiation-induced swelling under high-dose irradiation with He^{2+} ions, it was found that a decrease in grain size by 2.5 – 3 times leads to an increase in resistance to swelling and softening by 1.5 – 2 times. Moreover, for ZrO_2 ceramic samples obtained at grinding speeds of 700 – 900 rpm, strengthening is not only due to dimensional factors, but also to the structural ordering of the crystal lattice, due to thermal relaxation of residual mechanical stresses.

Keywords: Size effect; Zirconium dioxide; Ceramics; Radiation damage; Dislocation strengthening; Gas swelling
Received: 18 April 2024; Revised: 29 April 2024; Accepted: 15 May 2024.
Article type: Research article.

1. Introduction

Interest in radiation-resistant materials, as well as ways to increase their resistance to external influences through simple modification methods that do not require large costs and energy resources, has been most evident in the last decade, and is primarily due to the development of alternative energy, in which great emphasis is placed on new generation nuclear energy. At the same time, the most promising areas in nuclear energy are high-temperature nuclear reactors, as well as thermonuclear reactors, which can increase the efficiency of energy productivity, as well as increase the service life and burn-up of nuclear fuel through the use of more stable structural materials capable of withstanding prolonged exposure to radiation combined with high temperatures. The criteria of high radiation resistance, the ability to withstand high exposure temperatures, as well as maintain strength and thermophysical characteristics for a long time, are among the main ones when considering new types of materials as structural materials for new generation nuclear reactors.[1-6]

At the same time, much attention among structural materials for new generation nuclear reactors (including high-temperature ones) is given to ceramics. such as beryllium oxide (BeO),[7,8] zirconium dioxide (ZrO_2),[9,10] magnesium oxide (MgO),[11,12] aluminum magnesium spinel ($MgAl_2O_4$),[13-15] aluminum nitride (AlN),[16-18], silicon nitride (Si_3N_4),[19-21] silicon carbide (SiC)[21-23] tantalum carbide (TaC)[24] and their composite double or triple compounds.[25,26] Interest in these

[1] *Engineering Profile Laboratory, L.N. Gumilyov Eurasian National University, Satpayev St., Astana 010008, Kazakhstan.*
[2] *Laboratory of Solid-State Physics, The Institute of Nuclear Physics, Almaty 050032, Kazakhstan.*
[3] *Institute of Solid-State Physics, University of Latvia, 8 Kengaraga, LV-1063, Riga, Latvia.*
**Email:* kozlovskiy.a@inp.kz (A. L. Kozlovskiy)

types of ceramics, considered as structural materials, is primarily due to high strength indicators (about 1000 - 2000 HV), high melting temperature (for most ceramics $T_{melt} \sim 1700 - 2500$ °C), low thermal expansion when heated, as well as good insulating and dielectric characteristics. The prospects for using these types of ceramics as structural materials are covered in sufficient detail in fundamental works *W.J. Weber*,[1,2] *G. Was,*[3,4] *S. J. Zinkle*,[5,6] which describe in sufficient detail the prospects for using various types of ceramics as materials for the first wall of nuclear reactors, materials for creating dispersed nuclear fuel (as inert matrices or cer – cer materials), as materials used for long-term disposal of long-lived nuclear waste, *etc*. At the same time, much attention in these works is paid to the description of the mechanisms of radiation resistance of ceramics and their features in comparison with traditional metals and alloys, which are used today as structural materials in nuclear energy.[27,28] A distinctive feature of ceramics from metals and alloys when describing the mechanisms of radiation damage is their dielectric nature, which imposes certain restrictions on the migration cascade effects associated with the ionization of electrons during the interaction of incident ions with the crystal structure. These limitations are due to the dielectric characteristics of most refractory ceramics, which in the case of large values of energy transferred to the electronic subsystem of the damaged layer, which, as is known, leads to cascade effects of electron displacement, can lead to the formation of anisotropy of the electron density distribution due to the irreversible mechanism of electron displacement. In this case, the occurrence of anisotropy in the electron density distribution during high-dose irradiation can lead to a thermal effect associated with the formation of highly defective areas and structural distortions, which, when accumulated in the structure of the damaged layer, can lead to embrittlement and radiation erosion of the surface with its partial destruction.

Also, differences in radiation damage in ceramics and metals are also reflected in the case of high-dose irradiation with helium (He^{2+}), hydrogen (H^+) ions, leading to gas swelling processes associated with the effects of filling pores and voids with helium and hydrogen ions and subsequent deformation distortion of the surface layer, associated with a rise in gas-filled cavities, which, in the case of a sharp increase in the concentration of implanted ions, initiate processes of explosive destruction of the near-surface layer. In the case of metals, these effects occur at irradiation fluences of $10^{15} – 10^{17}$ ion/cm^2, while for ceramics, it has been established that the blister formation effect is observed at fluences of $10^{17} – 5\times10^{17}$ ion/cm^2. This difference in the effects of blister formation is associated with the structural features of ceramics, most of which are characterized by a hexagonal or monoclinic type of crystal structure, which lead to asymmetry of deformation distortions due to differences in the faces and, accordingly, a decrease in the rate of accumulation of structural distortions in the damaged layer with increasing irradiation fluence. Moreover, in the case of ceramics, unlike metals and alloys, radiation resistance is greatly influenced by effects associated with ionization processes that can lead to irreversible structural changes, such as amorphization and the formation of latent tracks,[29,30] polymorphic transformations associated with structural changes[31,32] a huge variety of point defects in different crystal sublattices[33-42] as well as deformation swelling and surface erosion.[43,44] In this regard, much attention for ceramic materials planned to be used as structural materials operating under conditions of increased background radiation is given to ways to enhance radiation resistance by adding stabilizing additives to the composition[45] and the formation of two-phase ceramics[46] or by changing the grain sizes in order to increase the dislocation density and create additional barriers to point and vacancy defects,[47] as well as implanted ions in the case of He^{2+} or H^+ irradiation.

The purpose of this study is to determine the effect of variation in grain sizes of ZrO_2 ceramics on resistance to radiation-induced swelling when irradiated with low-energy He^{2+} ions. The main hypothesis underlying this study is to determine the influence of changes in grain sizes, which can lead to additional boundary effects in the damaged layer of ceramics on radiation resistance and destruction processes associated with the accumulation of implanted He^{2+} under high-dose irradiation.

2. Materials and methods

Powders with a grain size of the order of 1.5 – 3 µm and a monoclinic type of crystal lattice were used as initial samples of ZrO_2 ceramics. These powders were purchased from Sigma Aldrich (Sigma, USA), the chemical purity of the samples in the initial state was 99.95 %.

Variation of the grain sizes of ZrO_2 ceramics was carried out by mechanochemical grinding (wet grinding method) in a planetary mill PULVERISETTE 7 premium line (Fritsch, Berlin, Germany) by changing the grinding speed from 300 to 900 rpm. To do this, samples of ZrO_2 powders were mixed with ethyl alcohol and placed in a 45 m EASY GTM grinding glass (zirconium dioxide material), in which balls with a diameter of 1.6 mm were used as grinding media. During grinding, changes in temperature and pressure in the grinding glass were monitored, which made it possible to evaluate the mechanisms occurring during grinding, as well as to evaluate the possibility of thermal heating of samples during crushing at high speeds. The grinding time was about 1 hour, after which the samples were removed from the glass and subjected to thermal annealing in a Nabertherm LE 4/11/R6 muffle furnace (Nabertherm, Lilienthal, Germany) at a temperature of 1500 °C for 5 hours, the heating rate was 20 °C/min, the samples were cooled together with the furnace for 24 hours after the annealing period had expired. The choice of annealing conditions and temperature is determined by the need to initiate the processes of thermal relaxation of mechanically induced deformation distortions that arise during the crushing of grains during grinding. In this case, the annealing temperature was selected experimentally in order to achieve the maximum effect of thermal relaxation of defects, while avoiding the effects of increasing grain growth during sintering. The choice of sample annealing temperature is based on a priori experimental work, according to which it was determined that at lower annealing temperatures the process of structural ordering occurs unevenly throughout the volume of annealed samples, and at higher temperatures the agglomeration effect dominates when grains are sintered into large agglomerates.

Determination of the grain sizes of the resulting ZrO_2 ceramics during their mechanochemical grinding and subsequent thermal annealing (used to relax mechanical deformation distortions) was carried out using the optical laser diffraction method implemented on an ANALYSETTE 22 NeXT Nano particle analyzer (Fritsch, Berlin, Germany). For this purpose, ceramic samples were dispersed in deionized water under the influence of ultrasound to obtain a stable suspension. The measurements were carried out in two ranges of green (0.1 - 45 μm) and red (45 - 2100 μm) lasers, the number of measurement passes was at least 3 for each sample. The results were presented in the form of particle size distribution diagrams depending on their weight contribution, as well as determined average values.

Determination of the morphological features of the synthesized ZrO_2 ceramics before and after mechanochemical grinding was carried out using scanning electron microscopy using a Phenom™ ProX microscope (Thermo Fisher Scientific, Eindhoven, the Netherlands). A dispersion method implemented using a Nebula particle disperser (Thermo Fisher Scientific, Eindhoven, the Netherlands) was used to uniformly distribute particles on the surface of the holders to eliminate the effects of particle aggregation.

Determination of structural changes associated with strain crushing during grinding and subsequent thermal annealing was performed using X-ray diffraction, implemented using a D8 ADVANCE ECO powder X-ray diffractometer (Bruker, Karlsruhe, Germany). X-ray diffraction patterns were obtained in the Bragg – Brentano geometry in the angular range 2θ = 20 - 75°, with a step of 0.03°. The shooting was carried out under conditions of constant rotation of the samples at a speed of 15 rpm. Determination of the crystal lattice parameters, as well as the magnitude of deformation distortions, was carried out using the Rietveld method, according to which the main quantities used for further calculations were calculated.

To conduct experiments on irradiation of ZrO2 ceramic samples in order to determine the mechanisms of radiation damage and destruction during the accumulation of damage and implantation of low-energy He^{2+} ions, the resulting samples in the form of powders were pressed into tablets with a thickness of about 10 μm and a diameter of 10 mm. Pressing was carried out in a special mold under a pressure of 200 MPa using a binder made from an aqueous solution of polyvinyl alcohol. After pressing, the resulting tablets were annealed at a temperature of about 700 °C for 3 hours to remove the binder and relieve the deformation stresses that arose during pressing. Experiments on irradiation of synthesized ZrO_2 ceramics were carried out at the DC-60 heavy ion accelerator, located in the Astana branch of the Institute of Nuclear Physics of the Ministry of Energy of the Republic of Kazakhstan (Astana, Kazakhstan). Low-energy He^{2+} ions with an energy of 40 keV (20 keV/charge) were used for irradiation; irradiation was carried out at fluences from 10^{15} to 5×10^{17} ion/cm^2. The choice of irradiation fluences is determined by the possibility of modeling the processes of accumulation of implanted ions in the near-surface layer, as well as the associated formation of gas-filled cavities, leading to swelling and subsequent destruction.

The determination of the penetration depth of ions in ceramics, as well as the dependence of the change in the ionization losses of incident ions as a result of elastic (dE/dx_{nuclei}) and inelastic collisions ($dE/dx_{electron}$) along the trajectory of ion movement in the material, was carried out by modeling interaction processes using the SRIM Pro 2013 code. The simulation results are presented in Fig. 1.

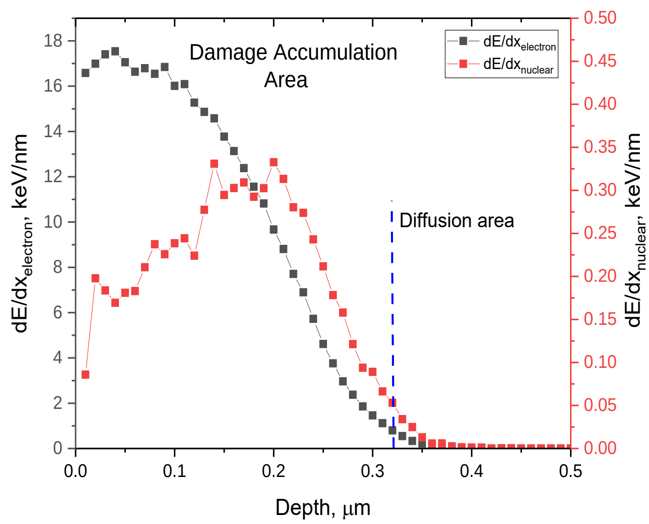

Fig. 1 Simulation results of ionization losses of incident He^{2+} ions in the surface layer of ZrO_2 ceramics (The dotted line on the graph indicates the boundary between the zone of main damage and the diffuse zone in which the accumulation of defects occurs as a result of diffusion).

As can be seen from the data presented, the maximum travel depth of He^{2+} ions in the surface layer of ceramics is about 330 - 400 nm, while this region is divided into the region of damage accumulation (with a depth of about 300 nm) and the region of possible diffusion of defects and implanted helium into the surface layer. The main contribution to the change in the properties of the near-surface damaged layer, according to modeling data, is made by inelastic collisions of incident ions with electrons ($dE/dx_{electron}$ value ~ 15 - 17 keV/nm), while the contribution from elastic collisions is less than 2-3 % (dE/dx_{nuclei} ~ 0.25 - 0.3 keV), which indicates that the main structural damage will be caused by athermal effects associated with the anisotropy of the electron density, and in the case of high-dose irradiation, effects associated with the accumulation of implanted helium and atomic displacements may appear. Moreover, in contrast to high-energy ions for which the $dE/dx_{electron}$ values are of the order of 25 - 26 keV/nm, ionization losses during irradiation with He^{2+} ions are no more than 65 - 70 % of the ionization losses of high-energy ions, which indicates a low probability of the occurrence of polymorphic transformations in the damaged layer, which have a clear dependence on the value of ionization losses of the incident ions, which determine the main mechanisms of radiation damage.

Determination of the influence of the accumulation of structural damage in the near-surface layer of ceramics after irradiation, and, as a consequence, the formation of deformation distortions, on changes in strength characteristics was carried out using the indentation method. This method was implemented on a Duroline M1 microhardness tester (Metkon, Bursa, Turkey), using a Vickers diamond pyramid as an indenter. The measurements were carried out by pressing the indenter with a constant load of 50 N on the surface of a ceramic sample, followed by holding it for 15 seconds and measuring the indenter print. Based on the measured diagonals of the imprint (in the form of a rhombus), the hardness values of the ceramic samples were determined. The measurements were carried out in the form of a series of 20 - 25 consecutive indentations, each subsequent indentation was spaced from the previous one by a distance of about 30 μm, which made it possible to avoid the influence of microcracks formed during indentation on the hardness measurement. The change in hardness (in the case of irradiated samples, characterizing the softening effect, in the case of initial samples with varying grain sizes, reflecting the hardening factor) depending on external factors (irradiation or changes in grain sizes) characterized the dynamics of changes in the strength characteristics of ceramics.

3. Results and discussion

As is known, the use of the mechanochemical grinding method (solid-phase synthesis method) makes it possible to initiate processes of structural changes and phase transformations as a result of mechanical action on samples and subsequent deformation distortion, which can lead to the formation of new phases by the type of introduction or substitution (if multicomponent ceramic compositions are used) or to initiate polymorphic transformations (changes in the polytype of the crystal structure). At the same time, varying the grinding conditions, including grinding time or speed, can control the synthesis processes, as well as determine the kinetics of the observed changes as a result of mechanical action (severe deformation of the structure). In the case of ZrO_2 ceramics with fairly high strength parameters (hardness of the order of 8 - 11 GPa) and phase transformation temperatures in the range of 1800 - 2500 °C (depending on the conditions of thermal exposure, as well as various stabilizing additives), the use of the method of mechanochemical solid-phase grinding is due to the possibilities of mechanical crushing of grains, without initializing the processes of phase transformations, as well as amorphization (strong structural disorder), characteristic of less hard types of ceramics.

Figures 2-3 show the results of the morphological features of ZrO_2 ceramics after mechanochemical grinding and thermal annealing. Morphological features were studied using

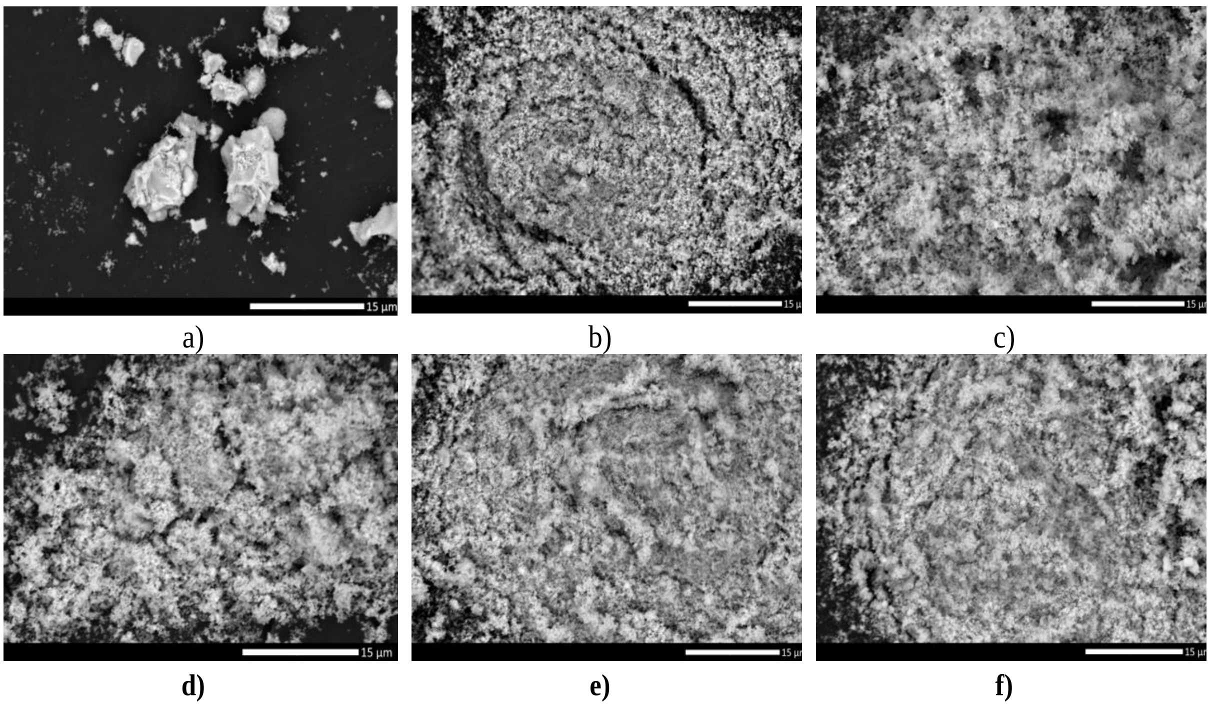

Fig. 2 Results of SEM images of ZrO_2 ceramics after mechanochemical grinding: a) initial; b) grinding at a speed of 300 rpm; c) grinding at a speed of 400 rpm; d) grinding at a speed of 500 rpm; e) grinding at a speed of 700 rpm; f) grinding at a speed of 900 rpm.

scanning electron microscopy (SEM); photographs were taken at the same magnification and scale to conduct a comparative analysis of changes in the size and shape of grains caused by external influences (mechanochemical grinding and subsequent thermal annealing).

In the case of the initial samples of ZrO_2 ceramics (not subjected to mechanochemical grinding), the samples are large-sized particles (1.5 - 3 μm), which has good agreement with the passport data. At the same time, the presence of smaller particles (the proportion of which is significantly smaller) causes a rather low adhesion of large grains to each other, due to the chemical processes of obtaining these particles. In the case of grinding, according to the data presented in electron micrographs (see Figs. 2b - f), there is a crushing of large grains into nano-sized particles with an irregular diamond-shaped or feather-like shape. At the same time, an increase in the grinding speed leads to smaller grains, which characterizes the fact that a more intense mechanical effect of the grinding bodies leads to faster crushing of grains and more intense grinding. Moreover, in the case of grinding speeds of 700 - 900 rpm, the formation of smaller agglomerates is observed, which is the combination of several grains into larger particles. This formation of agglomerates is due to effects associated with the properties of ZrO_2 powders upon transition to nanoscale scales.

The results of changes in the morphological features of ZrO_2 ceramics after thermal sintering presented in Fig. 3 indicate the agglomeration of grains into larger associations, in the form of fairly dense agglomerates consisting of fairly small grains (the size of which is about 200 - 400 nm, depending on the grinding speed), having a good correlation with the grain sizes of ceramics after mechanochemical grinding. Moreover, in the case of initial ceramics subjected to thermal annealing, a slight enlargement of grains is observed, associated with their sintering into larger agglomerates and compaction.

Figure 4 shows the results of size diagrams (grain size distribution diagrams) of ZrO_2 ceramics after mechanochemical grinding (Fig. 3a) and after thermal annealing (Fig. 3b). As can be seen, from the presented data on the size diagrams in the case of the original ZrO_2 ceramics, the distribution has two characteristic maxima in the region of 0.2 - 0.4 μm and 1.5 - 4 μm, characterizing the presence of large particles, as well as observed fragments in the form of a fine fraction (clearly visible in Fig. 3a). In the case of ZrO_2 ceramics subjected to mechanochemical grinding, the size diagrams are characterized by the presence of distributions in the region from 0.1 to 0.5 μm, having an almost symmetrical shape, indicating the absence of any large stable agglomerates that cannot be dispersed as a result of exposure to ultrasound (during dispersion for measuring dimensional diagrams).

For annealed particles, the size diagrams are characterized by two distributions in the region 0.1 - 0.5 μm and 1.0 - 50 μm (has two maxima for samples obtained at grinding speeds of 500 - 900 rpm). In this case, as shown in Fig. 3b, a distribution of 1.0 - 50 μm is characteristic of the resulting agglomerates (observed on the SEM image), consisting of small grains, the sizes of which are characterized by a distribution of 0.1 – 0.5 μm and have good agreement with the data of the distributions of samples obtained after grinding.

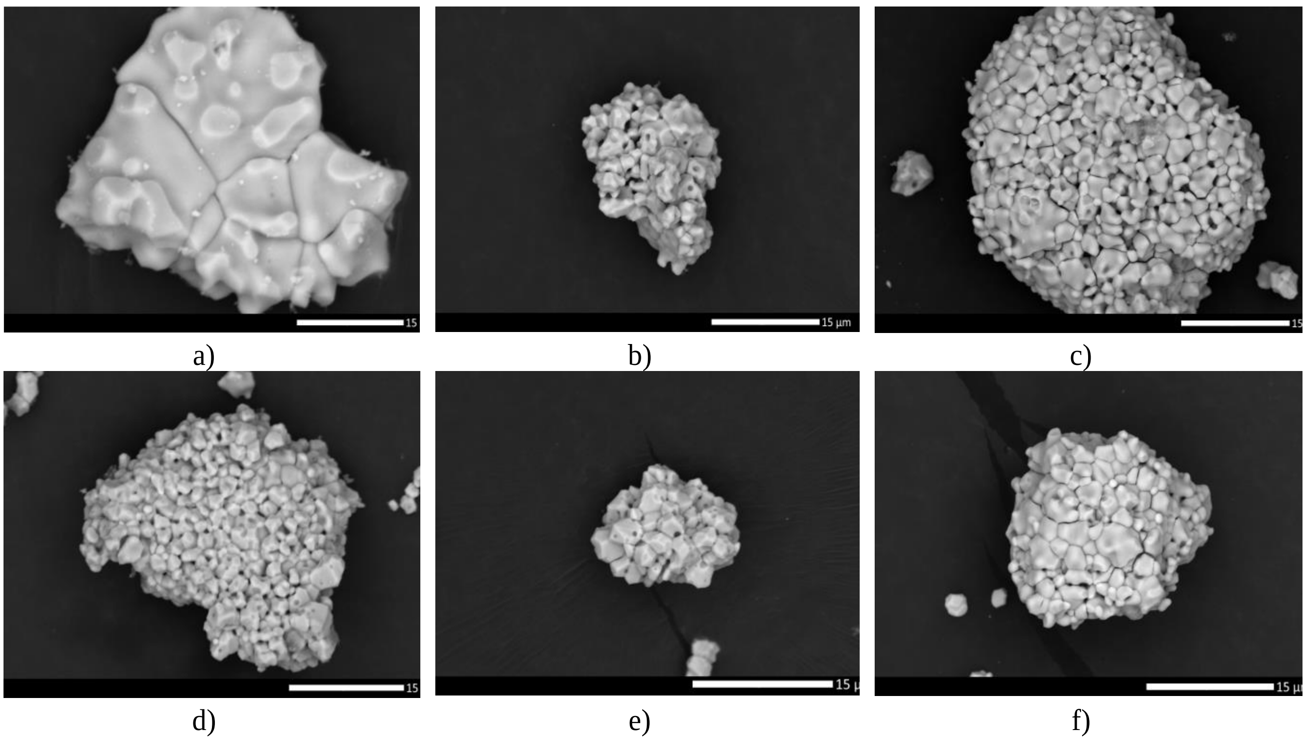

Fig. 3 Results of SEM images of ZrO_2 ceramics after mechanochemical grinding and thermal annealing at a temperature of 1500 °C: a) initial; b) grinding at a speed of 300 rpm; c) grinding at a speed of 400 rpm; d) grinding at a speed of 500 rpm; e) grinding at a speed of 700 rpm; f) grinding at a speed of 900 rpm.

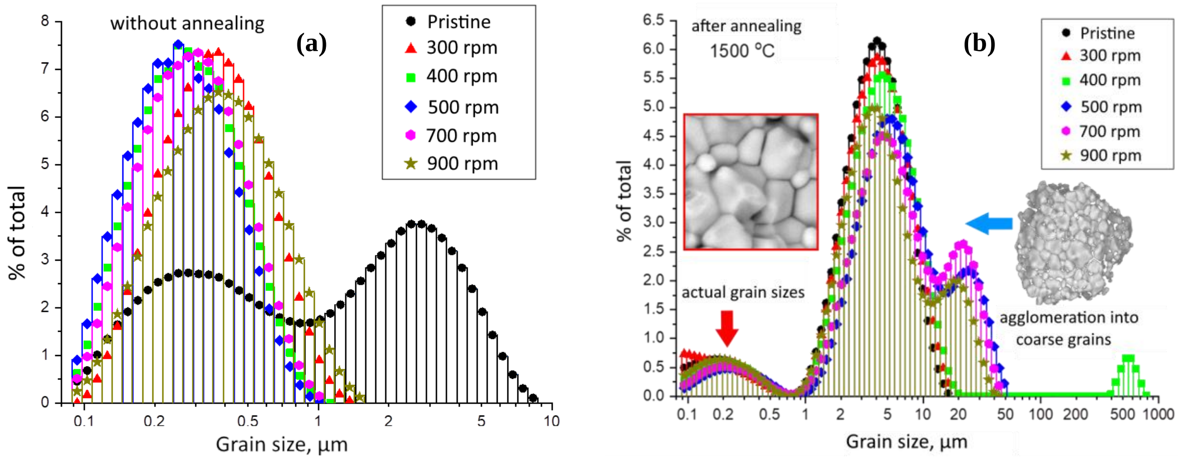

Fig. 4 Diagrams of grain size distribution of ZrO_2 ceramics depending on synthesis conditions: a) diagrams of grain size distribution after mechanochemical grinding; b) diagrams of grain size distribution after thermal annealing.

The presence of two distributions for ZrO_2 ceramics after thermal annealing has the following explanation. During thermal sintering of ground particles, the processes of their agglomeration are initialized with the formation of sufficiently strong agglomerates that cannot be broken up by dispersion in ultrasound. Moreover, these agglomerates are "assemblies" of nano-sized particles, the sizes of which are characteristic of mechanochemically ground ceramics (according to a comparison of electronic image data and distributions obtained using the laser optical diffraction method).

Figure 5a presents the results of changes in the average grain size determined using the laser optical diffraction method when assessing the distributions presented in Figs. 4a and 4b, taking into account the agglomeration of grains during thermal annealing into agglomerates (see Data presented in the SEM images). Calculations of the dislocation density and volumetric length of grain boundaries were performed using expressions (1) and (2) and are presented in Fig. 5b.

$$\delta = \frac{1}{D^2}, \tag{1}$$

$$f = \frac{3\vartheta(D-\vartheta)^2}{D^3}, \tag{2}$$

where D is the grain size, ϑ is the size of the grain boundary.

As can be seen from the presented data, in the case of the original ceramics, the average grain size is about 1.5 μm, which is in good agreement with the passport data for the original powders. Mechanochemical grinding at speeds of 300 - 400 rpm leads to a decrease in this size by about 2.5 - 3 times (350 - 380 nm), which indicates that the original powders are quite easily crushed when exposed to grinding media (i.e., low strength in the initial state). The observed increase in grain sizes at grinding speeds of the order of 700 - 900 rpm can be explained by the agglomeration of nano-sized grains subjected to severe deformation, which can initiate self-organization processes of fine particles. In fact, the observed effect of increasing grain size at high grinding speeds is due to the agglomeration properties of zirconia at small sizes, which leads to fine particles sticking together into larger agglomerates with a fairly developed surface. A decrease in particle size leads to an increase in dislocation density and volume fraction of grain boundaries (see Data in Fig. 4b), the values of which are inversely proportional to the grain size values. At the same time, an increase in the dislocation density and volume fraction of grain boundaries can lead to the effect of strengthening ceramics, due to the creation of additional

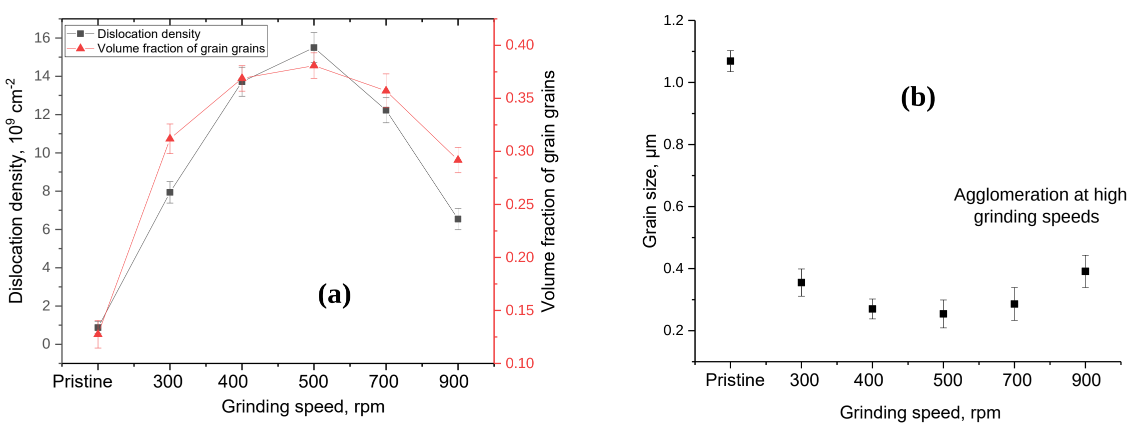

Fig. 5 Assessment results of the morphological parameters of ZrO_2 ceramics: a) Results of average grain size depending on grinding speed; b) Results of changes in dislocation density and volume fraction of grain boundaries depending on the grinding speed.

barriers to the propagation of microcracks under external influences, which reduces the rate of cracking and allows them to withstand higher loads. This effect can also be used to increase resistance to radiation damage during high-dose irradiation. In the case when the grain sizes in ceramics obtained at high grinding speeds form agglomerates, a decrease in dislocation density and volume fraction of grain boundaries is observed, since these values directly depend on the grain sizes. In this case, an increase in grain size due to their agglomeration into larger formations leads to enlargement of the boundaries, and as a consequence, a decrease in the dislocation density.

Figures 6a–b demonstrates the results of Raman spectroscopy of the studied ZrO_2 ceramics after mechanochemical grinding and thermal annealing, presented depending on the grinding speed in comparison with the original samples (before and after thermal annealing). The general appearance of the presented spectra of the studied ZrO_2 ceramics, depending on the conditions of mechanochemical grinding and subsequent thermal annealing, is characterized by the presence of a set of spectral lines (14 active modes) corresponding to the monoclinic phase of ZrO_2 A_g (178, 190, 305, 347, 475, 559, 638 cm^{-1}), 6 B_g (221, 333, 381, 503, 536, 615 cm^{-1}). At the same time, no changes associated with the appearance of new reflections indicating polymorphic phase transformations were detected either in the case of changes in the grinding speed during mechanochemical grinding or subsequent thermal annealing at a temperature of 1500 °C. The absence of such changes in the Raman spectra indicates the high resistance to polymorphic transformations of these ceramics to mechanical influences (during grain crushing), as well as their subsequent thermal annealing.

It should be noted that the main changes in the Raman spectra of the studied ZrO2 ceramics are observed for ground samples with increasing grinding speed, which are expressed in a shift in the position of the spectral lines and their broadening. Such changes indicate the accumulation of residual mechanical stresses in the structure, the appearance of which is associated with the processes of grain crushing. In this case, the most pronounced accumulation is observed for samples subjected to grinding at a speed of 700 - 900 rpm, for which the displacement is clearly expressed, and the very nature of changes in the position of spectral lines indicates the accumulation of tensile residual mechanical stresses in the structure.

In the case of annealed samples, practically no changes relative to the original sample (also annealed under the same conditions) are observed, which indicates the relaxation nature of structural changes associated with the thermal annihilation of residual mechanical stresses as a result of annealing of the samples. This nature of the changes indicates that the residual mechanical stresses induced by mechanical grinding are reversible (removed as a result of thermal annealing), while the grain sizes, according to these morphological features, do not undergo large changes associated with coarsening.

Figure 7 reveals the results of X-ray diffraction of the studied samples of ZrO_2 ceramics after grinding and thermal annealing, reflecting the phase composition of the studied ceramics, as well as changes in structural features depending on the conditions of exposure to the samples. The general appearance of the presented X-ray diffraction patterns in Figs. 7a and 7b, regardless of the grinding rate conditions, is characteristic of the monoclinic ZrO_2 phase with the spatial system P21/c(14). To identify the phase composition, tabular data from the PDF-2 (2016) database was used, which had a degree of agreement with experimentally obtained diffraction patterns of about 90 % (taking into account the deformation distortion of the crystal lattice, which affects the position of the diffraction reflections of the samples under study). To determine the parameters by refining them for the ceramics under study, a ZrO_2 (PDF-01-070-2491) card with a monoclinic crystal lattice type and parameters $a_0 = 5.1489$ Å, $b = 5.2180$ Å, $c = 5.3147$ Å, $\beta = 99.203°$, $V=140.78$ Å^3 was.

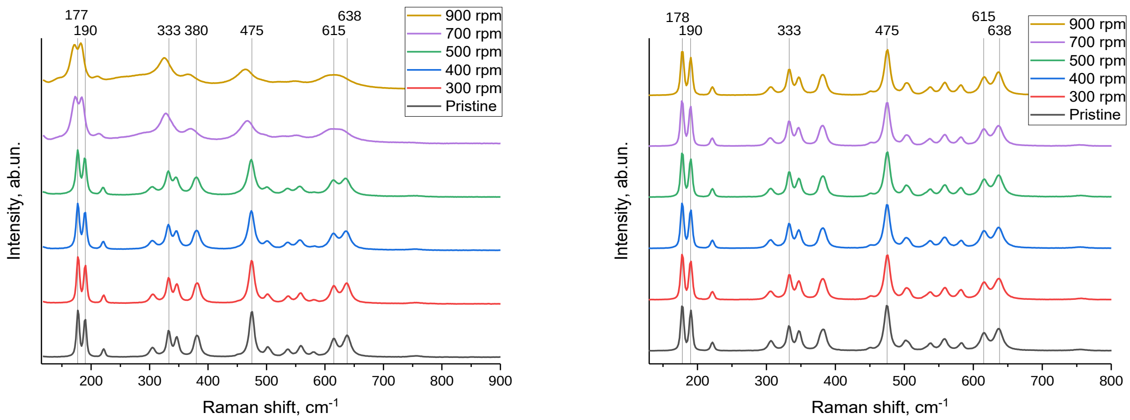

(a) (b)

Fig. 6 Results of Raman spectroscopy of the studied ZrO_2 ceramics (vertical lines display the positions of the maxima of the original sample, reflecting the effect of shifting the maxima, characterizing the deformation distortion of the structure): a) Raman spectra of ZrO_2 ceramics after mechanochemical grinding; b) Raman spectra of ZrO_2 ceramics after thermal annealing.

selected. The crystal lattice parameters were refined by approximation and subsequent calculation of the parameters according to the observed positions of diffraction reflections, taking into account their shape

As can be seen from the presented data on changes in the position of diffraction reflections of ceramic samples ground at a grinding speed of 300 - 400 rpm, the displacement of the reflections relative to the original sample is minimal, which indicates that grain fragmentation at these speeds occurs without severe deformations of the crystal structure. Also, the absence of pronounced changes in the intensity of diffraction reflections for these samples indicates the absence of processes of fragmentation of coherent scattering regions (crystallites). Increasing the grinding speed to 500-900 rpm leads to a more pronounced mixing of diffraction reflections relative to the initial position, which indicates the formation of deformation distortions in the structure caused by mechanical effects on the crystal structure. At the same time, an increase in the grinding speed leads to an increase in the observed displacement, and also at grinding speeds of 700 - 900 rpm, in addition to the displacement, a decrease in the intensity of diffraction reflections and an increase in shape asymmetry, characteristic of highly deformed structures, are observed.

According to the grinding control data (recording changes in pressure and temperature in the bowl), it was found that when the grinding speed was increased to 700 and 900 rpm

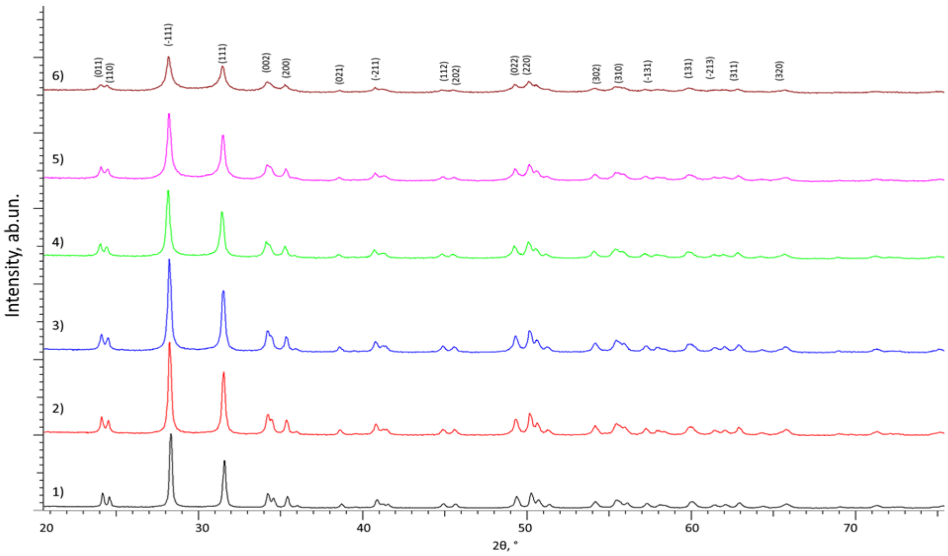

(a)

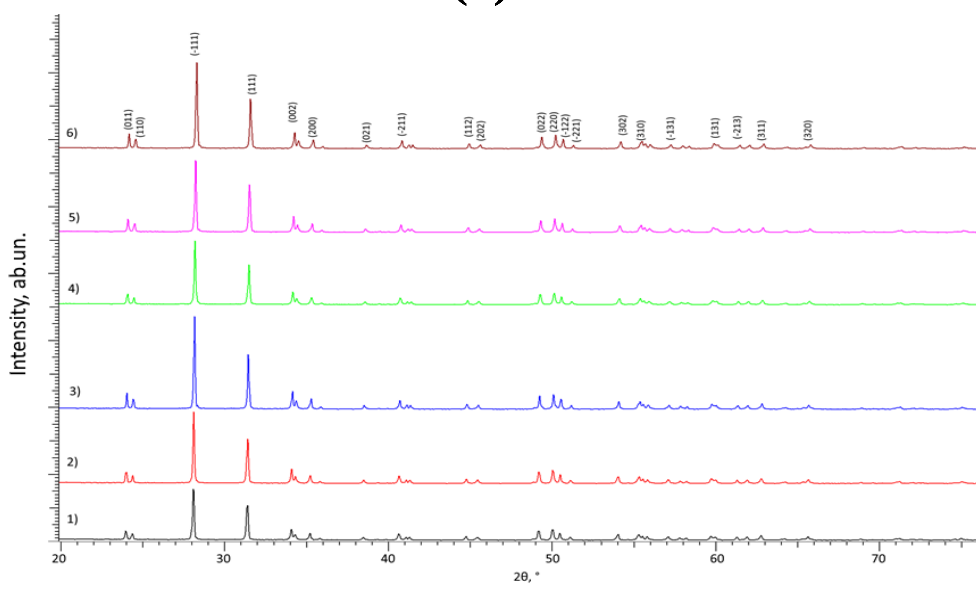

(b)

Fig. 7 Results of X-ray diffraction analysis of ZrO_2 ceramics: a) X-ray diffraction patterns of ZrO_2 ceramics after mechanochemical grinding; b) X-ray diffraction patterns of ZrO_2 ceramics after thermal annealing (1 – Pristine, 2 - 300 rpm, 3 - 400 rpm, 4 - 500 rpm, 5 - 700 rpm, 6 - 900 rpm).

during long-term grinding, an increase in the temperature inside the grinding bowl was observed to 48 - 50 °C and 65 - 67 °C, respectively. At the same time, the pressure inside the glass also increased to 1.5 - 2.5 bar. Such changes can be explained by the initialization of processes of accelerated deformation distortion of grains during their crushing, which is quite clearly visible when analyzing X-ray diffraction patterns of samples after mechanochemical grinding (diffraction reflections of the samples obtained during grinding at a speed of 900 rpm have a strongly pronounced asymmetric shape, as well as a large shift to the region of small angles, characteristic of deformation distortions of the structure).

Table 1 presents the results of structural parameter (parameters and volume of the crystal lattice) assessment of the studied ZrO_2 ceramics before and after mechanochemical grinding and thermal annealing. The determination of the parameters of the crystal lattice, as well as its volume, was carried out using the method of comparing the reference values of the position of diffraction lines and experimental ones. Based on the obtained displacement values, caused by both mechanical grinding and subsequent thermal exposure, deviations of the parameters from the reference values, which are characteristic of experimentally obtained samples, were established.

As can be seen from the data on changes in crystal lattice parameters presented in Table 1, thermal annealing of the original sample (not subjected to grinding) leads to a broadening of the parameters, which is due to the effects of thermal expansion of the crystal structure as a result of thermal exposure. Similar effects are observed for samples ground at a speed of 300 - 400 rpm, for which the general change in diffraction patterns in comparison with the original sample indicates a small influence of mechanochemical grinding on the deformation distortion of the crystal structure, and the values of the coefficient of thermal expansion ($\beta_V(T)$) for the samples in comparison with the change data for the original are of the order of 0.12×10^{-6} K^{-1}. In the case of samples ground at speeds of 500 - 900 rpm, the observed decrease in the crystal lattice parameters indicates the dominance of structural ordering processes as a result of thermal annealing of structural defects (including vacancy defects) over the thermal broadening of the crystal lattice caused by thermal vibrations. At the same time, the most pronounced changes are observed for samples ground at a grinding speed of 900 rpm, for which $\Delta V = 1.61$ Å^3 (not less than 1 %). This change in the volume of the crystal lattice, together with Raman spectroscopy data, indicates that the accumulation of residual mechanical stresses is directly related to the deformation swelling of the crystal structure, which relax as a result of thermal annealing under the selected annealing conditions.

Figure 8 shows the results of Williamson-Hall constructions (W-H constructions), reflecting the influence of dimensional factors (changes in the sizes of coherent scattering regions (crystallites)) and deformation factors (structural micro distortions of the crystal lattice) on the change in the FWHM (full width at half maximum) value of diffraction reflections depending on the diffraction angle. The general appearance of the presented dependences is characterized by the slope of the approximating straight line, the slope of which reflects the nature and magnitude of deformation distortions, as well as the value of the offset from 4sinθ along the βcosθ axis, which characterizes the change in the size factor (an increase or decrease in the size of crystallites depending on external conditions).

As can be seen from the presented data on the βcosθ - 4sinθ dependence when approximated for ZrO_2 ceramics after mechanochemical grinding, the main contribution to changes in the FWHM value in the case of grinding speeds of 300 – 500 rpm is made by tensile deformation distortions, the value of which is about 3 - 4×10^{-4}. The sizes of coherent scattering regions (crystallite size) for ZrO_2 ceramics obtained at these grinding speeds are about 40 - 45 nm and do not have obvious changes when the grinding speed increases from 300 to 500 rpm. In the case of grinding speeds of 700 - 900 rpm, a shift of the approximating straight lines is observed upward along the βcosθ axis, which indicates an increase in the size factor in the change in the FWHM value along with deformation distortions. Such a change in the W-H structures for ZrO_2 ceramic samples obtained at grinding speeds of 700 - 900 rpm

Table 1. Structural parameter data.

Type of exposure	Initial	Grinding speed, rpm				
		300	400	500	700	900
Mechanochemical grinding	a =5.1196 Å, b=5.1801 Å, c=5.3116 Å, β=99.203°, V=139.09 Å^3	a=5.1278 Å, b=5.1884 Å, c=5.3031 Å, β=99.262°, V=139.25 Å^3	a=5.1429 Å, b=5.1976 Å, c=5.3041 Å, β=99.204°, V=139.96 Å^3	a=5.1683 Å, b=5.1946 Å, c=5.3144 Å, β=99.299°, V=140.21 Å^3	a=5.1530 Å, b=5.1895 Å, c=5.3144 Å, β=99.220°, V=140.28 Å^3	a=5.1621 Å, b=5.1904 Å, c=5.3207 Å, β=99.221°, V=140.72 Å^3
Thermal annealing at 1500 °C	a=5.1583 Å, b=5.2199 Å, c=5.3295 Å, β=99.202°, V=141.65 Å^3	a=5.1419 Å, b=5.2334 Å, c=5.3206 Å, β=99.124°, V=141.36 Å^3	a=5.1509 Å, b=5.2159 Å, c=5.3268 Å, β=99.163°, V=142.22 Å^3	a=5.1437 Å, b=5.2056 Å, c=5.3105 Å, β=99.203°, V=140.16 Å^3	a=5.1407 Å, b=5.2056 Å, c=5.3083 Å, β=99.243°, V=140.21 Å^3	a=5.1196 Å, b=5.1801 Å, c=5.5137 Å, β=99.183°, V=139.11 Å^3

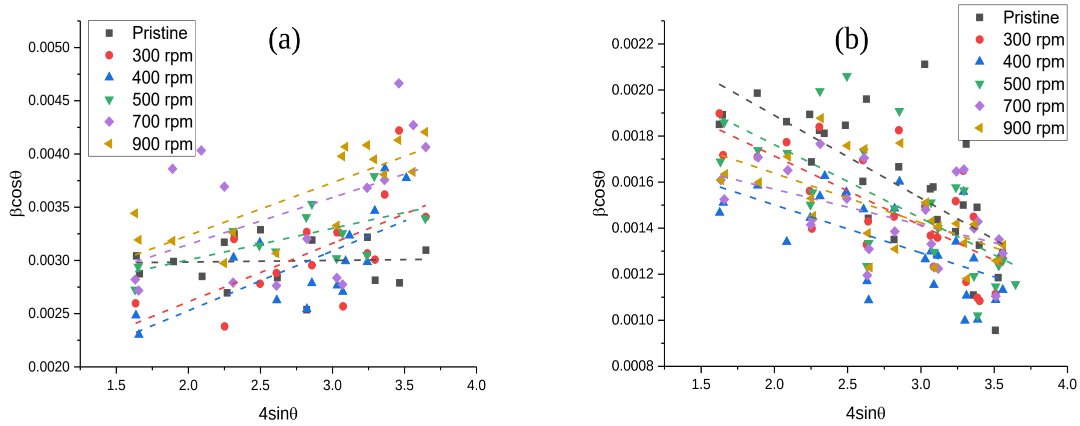

Fig. 8 Results of W-H constructions for the studied ZrO_2 ceramics: a) βcosθ - 4sinθ dependence for samples after grinding; b) βcosθ - 4sinθ dependence for samples after thermal annealing.

is characteristic of a decrease in the size of crystallites (as a result of intensive crushing) as well as an increase in deformation distortions characteristic of highly deformed structures (value $\varepsilon \sim 7 - 9\times10^{-4}$).

For ground samples of ZrO_2 ceramics subjected to thermal annealing, the nature of the dependences of the W-H plots is characteristic of the presence in the structure of the ceramics of compressive-type deformation distortions, the presence of which is characterized by relaxation processes caused by thermal exposure and subsequent agglomeration of grains (according to the results of morphological features). At the same time, the nature of agglomeration manifests itself not only at the macro level (in the form of the formation of agglomerates consisting of fine grains), but also at the crystalline level, expressed in the enlargement of coherent scattering regions (crystallites) from 70 - 75 nm (for initial annealed ZrO_2 ceramic samples) to 805 - 90 nm (for samples ground at a speed of 700 - 900 rpm and subjected to thermal annealing).

Such changes associated with a change in the type of deformation distortion from tensile (in the case of ground samples) to compression (in the case of annealed samples) indicate the relaxation nature of structural changes associated with thermal annealing of defects that arose during grinding. At the same time, an increase in the grinding speed from 500 to 700 - 900 rpm, according to W-H construction data, leads to more intense deformation of the crystal structure, characterized not only by structural distortion of the crystal lattice, but also by fragmentation of crystallites. At the same time, more pronounced deformation distortion of the crystal structure and fragmentation of crystallites during thermal annealing lead to more intense relaxation processes, changes in which, in combination with dimensional factors, can lead to an increase in strength characteristics, as well as thermophysical parameters.

Figure 9 demonstrates the assessment results of the hardness of the studied ZrO_2 ceramics after thermal annealing depending on the grinding speed. The graph also reveals the hardness value of the original sample before and after thermal annealing in order to reflect the influence of structural ordering on the change in the strength properties of the original ceramics, which, as was established when analyzing grain sizes using the laser optical diffraction method, after thermal annealing did not lend themselves to dispersion in an ultrasonic bath.

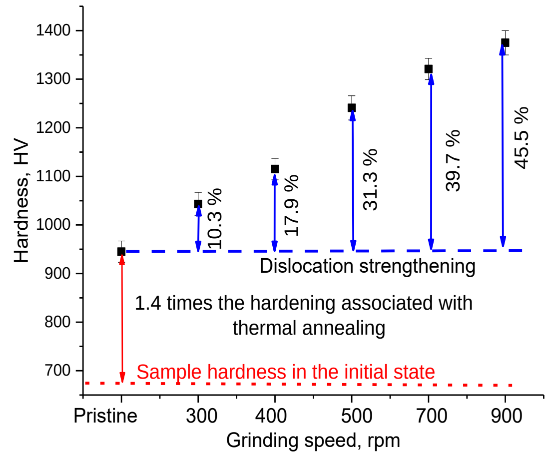

Fig. 9 Results of changes in the hardness of the surface layer of ZrO_2 ceramics depending on the production conditions (for comparison, the values of ZrO_2 ceramics samples in the initial state without annealing and subjected to thermal annealing are given).

The obtained hardness values for annealed ZrO_2 ceramics, depending on the production conditions (changes in the grinding speed), have characteristic values for ZrO_2 with a monoclinic type of crystal structure (baddeleyite type).[48] Moreover, the observed changes in hardness values in the case of varying production conditions (changes in grinding speed) indicate a positive influence of size factors on strengthening, characteristic of dislocation strengthening caused by changes in grain sizes.[49] The observed strengthening of ZrO_2 ceramics with changes in their grain sizes is in good agreement with the test data for determining the strength characteristics of nanostructured ZrO_2 presented.[50] At the same time, the established relationships between dimensional factors and hardening are in good agreement with the data determining the hardness and stress resistance of their work.[51] In fact, the strengthening effect directly depends on the dislocation density, as well as the degree of structural ordering that occurs during thermal annealing of the samples. In this case, dislocation strengthening is the dominant factor responsible for the high strength of the synthesized ceramics.

The problem of gas swelling (helium or hydrogen, in certain cases with the accumulation of a large amount of fission fragment products of nuclear fuel in the form of Kr or Xe) is one of the most important in the field of studying radiation defects and the influence of their evolution on the stability and operational stability of ceramic materials. In the case of high-energy irradiation, the problem of gas swelling is usually accompanied by the effects of deformation distortions associated with athermal processes caused by the transfer and subsequent dissipation of the energy of incident ions into the crystal structure of the irradiated material. Moreover, in the case of high-energy irradiation, these damages have a fairly large depth distribution (usually about 10 - 20 μm), which partially reduces the risks of intense deformation swelling of the surface layer due to the large thickness of the damaged layer (compared to low-energy irradiation). In turn, the high mobility of helium, the accumulation of which, as a rule, occurs in a small near-surface layer (thickness of the order of 0.3 - 1.0 μm) can have a significant impact on the agglomeration and subsequent destruction of the near-surface layer of ceramics. The accumulation of helium in the near-surface layer of structural materials can occur as a result of α-decay of actinides during long-term storage or operation of structural materials, and due to high mobility and low solubility, as well as the ability to agglomerate in voids with the subsequent formation of gas-filled bubbles, it can have a negative effect on the destruction of the surface layer. Helium itself is quite capable of being captured by vacancies formed as a result of athermal processes and the knocking out of atoms during irradiation, which in turn leads to the formation of composite clusters of the He-V type, which subsequently become centers of nucleation of gas-filled helium bubbles.

According to the assessment of changes in X-ray diffraction patterns of the studied samples of ZrO_2 ceramics in comparison with the irradiation fluence, it was established that there are no effects associated with polymorphic transformations caused by irradiation, which indicates that during low-energy irradiation with He^{2+} ions, the polymorphic transformation processes are not initiated. The observed effects associated with the absence of polymorphic transformations in the damaged layer of ZrO_2 ceramics indicate that the main role in polymorphic transformations during ion irradiation is played by the values of transferred energy during elastic and inelastic interactions (for He^{2+} ions $dE/dx_{electron}$ = 15 - 17 keV/nm, and in the case of high-energy Xe ions $dE/dx_{electron}$ = 23 - 27 keV/nm (data from works,[52-54] for which the effects of polymorphic transformations were observed), and not by the deformational nature of structural changes associated with an increase in the concentration of defects in the structure of the damaged layer. In this case, when irradiated with He^{2+} ions, even when displacements of the order of 6 - 10 dpa are achieved, the main role in changing the properties of ceramics is played by deformation effects associated with the accumulation of structural distortions (tensile type), as well as volumetric swelling of the crystal lattice during its deformation.

Figure 10a presents the results of a comparative analysis of changes in the volumetric swelling of the crystal lattice of the studied samples of ZrO_2 ceramics, determined by assessing changes in the structural parameters and volume of the crystal lattice. The effect of gas swelling was assessed based on the results of a comparative analysis of the deformation volumetric distortion of the crystal structure of the damaged layer in ceramics depending on the irradiation fluence. For this purpose, X-ray diffraction patterns of the samples were measured before and after irradiation, on the basis of which results were obtained for the volume of the crystal lattice depending on the irradiation fluence. Based on these volumes, the effect of gas volumetric swelling was determined.

This value characterizes changes in the crystal structure of ceramics that occur during irradiation with He^{2+} ions, which is accompanied by processes of accumulation of structural distortions associated with a thermal effect caused by ionization energy losses along the trajectory of incident ions during interaction with the target.

As can be seen from the presented data on changes in the magnitude of swelling (volumetric swelling of the crystal lattice), in the case of small doses this value practically does not appear, which indicates the small influence of swelling on structural changes in the damaged layer. The most pronounced changes in volumetric swelling are observed at displacement values of the order of 5 - 6 dpa, which corresponds to a fluence of 10^{17} ion/cm^2. The observed increase in the swelling value at these fluences is in good agreement with literature data[55,56] indicating that the processes of swelling of the near-surface layer occur when fluences reach above 10^{17} ion/cm^2, which are characterized by fairly high concentrations of implanted helium ions in the near-surface layer. In the case of ZrO_2 ceramics, according to simulation calculations in SRIM Pro presented in Section 2, for fluences above 10^{17} ion/cm^2, implanted helium concentrations of the order of 1-5 at. % are characteristic, the concentrations of which are characteristic of the formation of gas-filled bubbles.

Figure 10b shows the results of changes in hardness depending on the amount of damage (atomic displacements) in the damaged layer of ZrO_2 ceramics obtained under different grinding conditions. The general trend of changes in hardness indicates a fairly high resistance of ZrO_2 ceramics to softening, up to atomic displacements of the order of 1 dpa (irradiation fluence of the order of 10^{17} ion/cm^2), while, as in

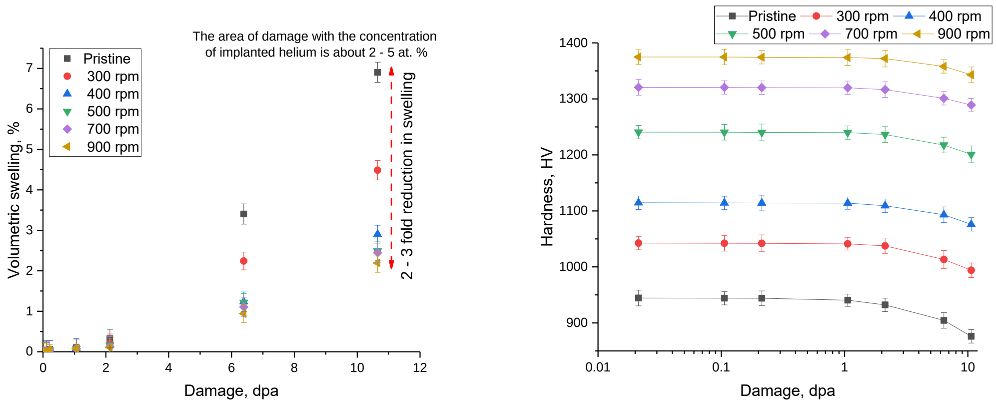

(a) (b)

Fig. 10 a) Results of the assessment of radiation-induced volumetric structural swelling of the near-surface layer as a result of high-dose irradiation with He^{2+} ions; b) Results of changes in the hardness of ZrO_2 ceramics with increasing irradiation fluence.

the case of changes in structural parameters (volumetric swelling), the change in hardness has a clear dependence on the concentration of implanted helium in the surface layer, an increase in which is accompanied (according to the data presented in Fig. 11a)) by volumetric swelling (accumulation of tensile-type deformation stresses). It should also be noted that the change in hardness for ZrO_2 ceramics depending on the magnitude of atomic displacements also has a clearly pronounced character associated with dimensional factors (i.e., changes in grain sizes with changes in the grinding speed of ceramics). In this case, a decrease in grain size leads to a less pronounced decrease in hardness under high-dose irradiation, the change of which is less than 2 - 3 % for samples obtained at grinding speeds of 700 - 900 rpm. This effect, as in the case of changes in structural parameters, is due to higher dislocation density for ground samples of ZrO_2 ceramics, an increase in which leads to the creation of additional barriers and, as a consequence, increased resistance to both swelling and softening.

One of the most indicative characteristics that determine the kinetics of radiation damage depending on the irradiation fluence (or the magnitude of atomic displacements) is a comparison of the dependences of structural swelling (increase in the volume of the crystal lattice) and softening (decrease in the hardness of irradiated samples). The degree of softening was assessed by comparing the hardness results of the samples before and after irradiation, on the basis of which a decrease in hardness was determined due to the cumulative effect associated with deformation swelling. These dependencies show the relationship between structural changes caused by deformation distortions and disorder with changes in strength characteristics, the decrease of which indicates the negative impact of accumulated deformation distortions on radiation resistance. The results of the comparative analysis are presented in Figure 11.

The presented dependence of the comparison of changes in the values of swelling and softening of ZrO_2 ceramics with increasing irradiation fluence (the magnitude of atomic displacements) shows a good correlation between changes in structural degradation and a decrease in strength properties, which are most pronounced at high irradiation fluences. At the same time, the order of magnitude of swelling and softening is approximately equal, which indicates that the main role in reducing strength properties under high-dose irradiation is played by effects associated with the accumulation of implanted helium in the surface layer, leading to swelling, as a result of which a large density of deformation distortions and stresses is formed in the near-surface layer. At the same time, analyzing the data obtained, we can conclude that a decrease in grain sizes due to crushing of the original ceramic samples leads to an increase in resistance to swelling and softening by more than 1.5 - 2 times. Moreover, the more intense the grinding speed, which leads not only to crushing, but also to structural changes in the original samples, the higher the resistance to radiation-induced degradation (helium swelling). This effect can be explained not only by dimensional factors that determine the occurrence of the dislocation strengthening effect, but also by structural modifications as a result of the deformation effect on the crystal lattice and its subsequent thermally induced relaxation, leading to ordering and compaction (see data on changes in the crystal lattice volume from Table 1).

Thus, by analyzing the obtained dependences of changes in structural characteristics (volumetric swelling of the crystal lattice) and softening (decrease in hardness depending on irradiation fluence), it can be concluded that dimensional factors have a positive influence, leading to strengthening and increasing the resistance of ZrO_2 ceramics to gas swelling associated with high-dose irradiation. The increase in the resistance of ceramics to external influences, as well as increased resistance to cracking due to the accumulation of structural distortions in the event of irradiation, is due to nanoscale effects associated with small grain sizes, as well as high dislocation density, an increase in which with decreasing grain sizes leads to the formation of additional limiting factors, having a positive effect on increasing resistance to external

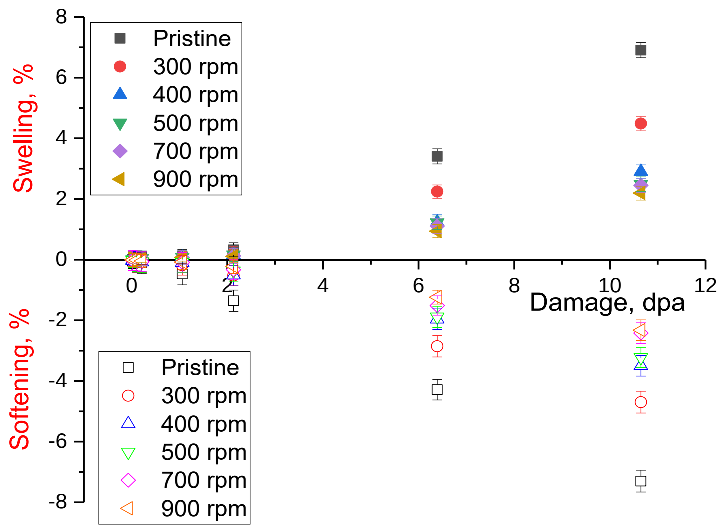

Fig. 11 Results of a comparative analysis of swelling and softening of ZrO_2 ceramics depending on the value of displacements.

influences. Similar effects characteristic of dislocation strengthening in the case of nano-sized ceramics were also previously shown in works.[57,58]

4. Conclusion

During the studies of the influence of mechanochemical grinding conditions on the change in dimensional factors in ZrO_2 ceramics, it was found that increasing the grinding speed from 300 to 900 rpm does not lead to the initiation of polymorphic transformation processes of the m-ZrO_2 → t-ZrO_2 type, which are also not initiated during thermal annealing of samples at a temperature of 1500 °C, the choice of which was due to thermal relaxation of structural deformation distortions caused by mechanochemical grinding during grain crushing. During the analysis of the obtained X-ray diffraction patterns of ZrO_2 ceramic samples after grinding and subsequent thermal annealing, it was established that during grinding, the dominant factor in structural changes at low grinding speeds is deformation tensile distortions, while at grinding speeds of 700 - 900 rpm, a certain role in changing the structural characteristics, in addition to deformation tensile distortions, is played by dimensional factors associated with a decrease in coherent scattering regions. In the case of thermal annealing, the main mechanism of structural changes is associated with relaxation ordering of the crystal structure through the dominance of compressive stresses. Moreover, more pronounced structural changes at high grinding speeds (at 700 - 900 rpm) lead to more intense structural ordering, accompanied by processes of crystallite enlargement. It has been established that a change in grain size, leading to an increase in the dislocation density and volume fraction of grain boundaries, leads to strengthening of ZrO_2 ceramics (increase in hardness), which is about 17 - 40% compared to the initial hardness value for annealed ZrO_2 ceramics (without mechanochemical effects). It has been determined that in the case of irradiation with low-energy He^{2+} ions, the processes of polymorphic transformations of the m-ZrO_2 → t-ZrO_2 type are not established, which confirms the data on the influence of the values of ionization electron losses ($dE/dx_{electron}$) on the polymorphic transformation processes in zirconium dioxide. In determining the influence of size effects (dislocation strengthening) on the resistance of ZrO_2 ceramics to radiation-induced swelling under high-dose irradiation with He^{2+} ions, it was found that a decrease in grain size by 2.5 - 3 times leads to an increase in resistance to swelling and softening by 1.5 - 2 times.

Acknowledgment

This research was funded by the Science Committee of the Ministry of Education and Science of the Republic of Kazakhstan (No. BR18574135). In addition, M. K and A.I.P. were supported by EUROfusion Enabling Research Project ENR-MAT.02.ISSP-UL- "New dielectric functional materials and interfaces (DFMI) – Theoretical and Experimental analysis." This work has been carried out within the framework of the EUROfusion Consortium, funded by the European Union via the Euratom Research and Training Programme (Grant Agreement No 101052200 — EUROfusion). Views and opinions expressed are however those of the author(s) only and do not necessarily reflect those of the European Union or the European Commission. Neither the European Union nor the European Commission can be held responsible for them. The research was performed in the Center of Excellence of the Institute of Solid-State Physics, University of Latvia, supported through European Unions Horizon 2020 Framework Programme H2020-

WIDESPREAD-01-2016-2017-TeamingPhase2 under grant agreement No. 739508, project CAMART2.

Conflict of Interest

There is no conflict of interest.

Supporting Information

Not applicable.

References

[1] Y. Zhang, W. J. Weber, Ion irradiation and modification: the role of coupled electronic and nuclear energy dissipation and subsequent nonequilibrium processes in materials, *Applied Physics Reviews*, 2020, **7**, 041307, doi: 10.1063/5.0027462.
[2] W. J. Weber, Models and mechanisms of irradiation-induced amorphization in ceramics, *Nuclear Instruments and Methods in Physics Research Section B: Beam Interactions with Materials and Atoms*, 2000, **166-167**, 98-106, doi: 10.1016/s0168-583x(99)00643-6.
[3] G. S. Was, Fundamentals of radiation materials science: metals and alloys Berlin: Springer, 2007.
[4] S. J. Zinkle, G. S. Was, Materials challenges in nuclear energy, *Acta Materialia*, 2013, **61**, 735-758, doi: 10.1016/j.actamat.2012.11.004.
[5] S. J. Zinkle, J. T. Busby, Structural materials for fission & fusion energy, *Materials Today*, 2009, **12**, 12-19, doi: 10.1016/s1369-7021(09)70294-9.
[6] S. J. Zinkle, L. L. Snead, Designing radiation resistance in materials for fusion energy, *Annual Review of Materials Research*, 2014, **44**, 241-267, doi: 10.1146/annurev-matsci-070813-113627.
[7] M.-D. Hou, X.-W. Zhou, B. Liu, Beryllium oxide utilized in nuclear reactors: part II, A systematic review of the neutron irradiation effects, *Nuclear Engineering and Technology*, 2023, **55**, 408-420, doi: 10.1016/j.net.2022.10.020.
[8] M.-D. Hou, X.-W. Zhou, B. Liu, Beryllium oxide utilized in nuclear reactors: part I: Application history, thermal properties, mechanical properties, corrosion behavior and fabrication methods, *Nuclear Engineering and Technology*, 2022, **54**, 4393-4411, doi: 10.1016/j.net.2022.07.017.
[9] D. V. Ananchenko, S. V. Nikiforov, K. V. Sobyanin, S. F. Konev, A. K. Dauletbekova, G. Akhmetova-Abdik, A. T. Akilbekov, A. I. Popov, Paramagnetic defects and thermoluminescence in irradiated nanostructured monoclinic zirconium dioxide, *Materials*, 2022, **15**, 8624, doi: 10.3390/ma15238624.
[10] S. Nikiforov, A. Dauletbekova, M. Gerasimov, Y. Kasatkina, O. Denisova, V. Lisitsyn, M. Golkovski, A. Akylbekova, A.-D. Bazarbek, A. Akilbekov, A. I. Popov, Thermoluminescent and dosimetric properties of zirconium dioxide ceramics irradiated with high doses of pulsed electron beam, *Crystals*, 2023, **13**, 1585, doi: 10.3390/cryst13111585.
[11] X. Jin, A. Boulle, J. Bourçois, A. Debelle, Comparison of neutron and ion irradiation induced lattice parameter changes in Ni and MgO single crystals, *Journal of Nuclear Materials*, 2021, **557**, 153308, doi: 10.1016/j.jnucmat.2021.153308.
[12] M. A. Monge, R. González, J. E. Muñoz Santiuste, R. Pareja, Y. Chen, E. A. Kotomin, A. I. Popov, Photoconversion of F+ centers in neutron-irradiated MgO, *Nuclear Instruments and Methods in Physics Research Section B: Beam Interactions with Materials and Atoms*, 2000, **166-167**, 220-224, doi: 10.1016/s0168-583x(99)00751-x.
[13] E. Shablonin, I. Kudryavtseva, A. I. Popov, V. Seeman, E. Vasil'chenko, A. Lushchik, Thermal annealing of lattice defects in $MgAl_2O_4$ single crystals irradiated by swift heavy ions, *Journal of Nuclear Materials*, 2024, **590**, 154874, doi: 10.1016/j.jnucmat.2023.154874.
[14] H. Klym, I. Karbovnyk, S. Piskunov, A. I. Popov, Positron annihilation lifetime spectroscopy insight on free volume conversion of nanostructured $MgAl_2O_4$ ceramics, *Nanomaterials*, 2021, **11**, 3373, doi: 10.3390/nano11123373.
[15] A. Akilbekov, A. Kiryakov, A. Dauletbekova, G. Aralbayeva, A. Akylbekova, Z. Ospanova, Unveiling the structural and optical properties of $MgAl_2O_4$ single crystals irradiated by swift heavy ions, *Materials*, 2024, **17**, 344, doi: 10.3390/ma17020344.
[16] Y. V. Bikhert, A. L. Kozlovskiy, A. I. Popov, M. V. Zdorovets, Study of the relationship between changes in the structural, optical, and strength properties of AlN ceramics subjected to irradiation with heavy Xe^{23+} ions, *Materials*, 2023, **16**, 6362, doi: 10.3390/ma16196362.
[17] Y. V. Bikhert, A. L. Kozlovskiy, A. I. Popov, M. V. Zdorovets, Study of the influence of the irradiation flux density on the formation of a defect structure in AlN in the case of the effect of overlapping of the heavy ion motion trajectories in the near-surface layer, *Materials*, 2023, **16**, 5225, doi: 10.3390/ma16155225.
[18] T. Yano, Y. Futamura, M. Imai, K. Yoshida, Recovery behavior of neutron-induced damage of AlN irradiated at higher temperatures by thermal annealing, *Journal of Nuclear Materials*, 2013, **440**, 495-499, doi: 10.1016/j.jnucmat.2013.02.025.
[19] A. Zhumazhanova, A. Mutali, A. Ibrayeva, V. Skuratov, A. Dauletbekova, E. Korneeva, A. Akilbekov, M. Zdorovets, Raman study of polycrystalline Si_3N_4 irradiated with swift heavy ions, *Crystals*, 2021, **11**, 1313, doi: 10.3390/cryst11111313.
[20] M. Romanova, L. Avotina, M. Andrulevicius, Y. Dekhtyar, G. Enichek, G. Kizane, M. Novotný, E. Pajuste, P. Pokorný, T. Yager, A. Zaslavski, Radiation resistance of nanolayered silicon nitride capacitors, *Nuclear Instruments and Methods in Physics Research Section B: Beam Interactions with Materials and Atoms*, 2020, **471**, 17-23, doi: 10.1016/j.nimb.2020.03.010.
[21] T. Yano, M. Akiyoshi, K. Ichikawa, Y. Tachi, T. Iseki, Physical property change of heavily neutron-irradiated Si_3N_4 and SiC by thermal annealing, *Journal of Nuclear Materials*, 2001, **289**, 102-109, doi: 10.1016/s0022-3115(00)00688-7.
[22] Y. Katoh, T. Nozawa, L. L. Snead, K. Ozawa, H. Tanigawa, Stability of SiC and its composites at high neutron fluence, *Journal of Nuclear Materials*, 2011, **417**, 400-405, doi: 10.1016/j.jnucmat.2010.12.088.
[23] H. Wang, T. Koyanagi, J. W. Geringer, A. A. Campbell, Y. Katoh, Determination of neutron irradiation temperatures of SiC using electrical resistivity method, *Journal of Nuclear Materials*,

2020, **540**, 152370, doi: 10.1016/j.jnucmat.2020.152370.
[24] J. Morillo, C. H. de Novion, J. Dural, Neutron and electron radiation defects in titanium and tantalum monocarbides: an electrical resistivity study, *Radiation Effects*, 1981, **55**, 67-77, doi: 10.1080/00337578108225467.
[25] D. J. Tallman, L. He, J. Gan, E. N. Caspi, E. N. Hoffman, M. W. Barsoum, Effects of neutron irradiation of Ti_3SiC_2 and Ti_3AlC_2 in the 121–1085°C temperature range, *Journal of Nuclear Materials*, 2017, **484**, 120-134, doi: 10.1016/j.jnucmat.2016.11.016.
[26] A. L. Kozlovskiy, D. I. Shlimas, M. V. Zdorovets, E. Elsts, M. Konuhova, A. I. Popov, Investigation of the effect of PbO doping on telluride glass ceramics as a potential material for gamma radiation shielding, *Materials*, 2023, **16**, 2366, doi: 10.3390/ma16062366.
[27] G. Meric de Bellefon, J. C. van Duysen, Tailoring plasticity of austenitic stainless steels for nuclear applications: review of mechanisms controlling plasticity of austenitic steels below 400°C, *Journal of Nuclear Materials*, 2016, **475**, 168-191, doi: 10.1016/j.jnucmat.2016.04.015.
[28] N. Sridharan, M. N. Gussev, K. G. Field, Performance of a ferritic/martensitic steel for nuclear reactor applications fabricated using additive manufacturing, *Journal of Nuclear Materials*, 2019, **521**, 45-55, doi: 10.1016/j.jnucmat.2019.04.020.
[29] A. Janse van Vuuren, A. Ibrayeva, R. A. Rymzhanov, A. Zhalmagambetova, J. H. O'Connell, V. A. Skuratov, V. V. Uglov, S. V. Zlotski, A. E. Volkov, M. Zdorovets, Latent tracks of swift Bi ions in Si_3N_4, *Materials Research Express*, 2020, **7**, 025512, doi: 10.1088/2053-1591/ab72d3.
[30] B. Canut, A. Ayari, K. Kaja, A.-L. Deman, M. Lemiti, A. Fave, A. Souifi, S. Ramos, Ion-induced tracks in amorphous Si_3N_4 films, *Nuclear Instruments and Methods in Physics Research Section B: Beam Interactions with Materials and Atoms*, 2008, **266**, 2819-2823, doi: 10.1016/j.nimb.2008.03.125.
[31] M. Alin, A. L. Kozlovskiy, M. V. Zdorovets, V. V. Uglov, Study of the mechanisms of the t-ZrO_2 → c-ZrO_2 type polymorphic transformations in ceramics as a result of irradiation with heavy Xe^{22+} ions, *Solid State Sciences*, 2022, **123**, 106791, doi: 10.1016/j.solidstatesciences.2021.106791.
[32] A. G. Balogh, Irradiation induced defect formation and phase transition in nanostructured ZrO_2, *Nuclear Instruments and Methods in Physics Research Section B: Beam Interactions with Materials and Atoms*, 2012, **282**, 48-58, doi: 10.1016/j.nimb.2011.08.063.
[33] G. Baubekova, A. Akilbekov, E. Feldbach, R. Grants, I. Manika, A. I. Popov, K. Schwartz, E. Vasil'chenko, M. Zdorovets, A. Lushchik, Accumulation of radiation defects and modification of micromechanical properties under MgO crystal irradiation with swift 132Xe ions, *Nuclear Instruments and Methods in Physics Research Section B: Beam Interactions with Materials and Atoms*, 2020, **463**, 50-54, doi: 10.1016/j.nimb.2019.11.021.
[34] G. Baubekova, A. Akilbekov, E. A. Kotomin, V. N. Kuzovkov, A. I. Popov, E. Shablonin, E. Vasil'chenko, M. Zdorovets, A. Lushchik, Thermal annealing of radiation damage produced by swift 132Xe ions in MgO single crystals, *Nuclear Instruments and Methods in Physics Research Section B: Beam Interactions with Materials and Atoms*, 2020, **462**, 163-168, doi: 10.1016/j.nimb.2019.11.013.
[35] A. Lushchik, V. Seeman, E. Shablonin, E. Vasil'chenko, V. N. Kuzovkov, E. A. Kotomin, A. I. Popov, Detection of hidden oxygen interstitials in neutron-irradiated corundum crystals, *Optical Materials: X*, 2022, **14**, 100151, doi: 10.1016/j.omx.2022.100151.
[36] D. Nesheva, Electron and neutron beam irradiation effects in homogeneous and nanostructured oxides, *ACS Omega*, 2023, **8**, 12603-12612, doi: 10.1021/acsomega.3c00486.
[37] N. Mironova-Ulmane, A. I. Popov, G. Krieke, A. Antuzevics, V. Skvortsova, E. Elsts, A. Sarakovskis, Low-temperature studies of Cr^{3+} ions in natural and neutron-irradiated g-Al spinel, *Low Temperature Physics*, 2020, **46**, 1154-1159, doi: 10.1063/10.0002467.
[38] M. Haseman, C. B. Somodi, P. Stepanov, D. E. Wall, L. A. Boatner, P. Hosemann, Y. Q. Wang, B. P. Uberuaga, F. A. Selim, Neutron irradiation induced defects in oxides and their impact on the oxide properties, *Journal of Applied Physics*, 2021, **129**, 215901, doi: 10.1063/5.0046292.
[39] R. Rasmidi, M. Duinong, F. P. Chee, Radiation damage effects on zinc oxide (ZnO) based semiconductor devices–a review, *Radiation Physics and Chemistry*, 2021, **184**, 109455, doi: 10.1016/j.radphyschem.2021.109455.
[40] R. Hazem, M. Izerrouken, Proton irradiation-induced defect aggregation and metallic nanoparticles in CaF_2 single-crystal, *Radiation Physics and Chemistry*, 2023, **204**, 110643, doi: 10.1016/j.radphyschem.2022.110643.
[41] Z. T. Karipbayev, K. Kumarbekov, I. Manika, A. Dauletbekova, A. L. Kozlovskiy, D. Sugak, S. B. Ubizskii, A. Akilbekov, Y. Suchikova, A. I. Popov, Optical, structural, and mechanical properties of $Gd_3Ga_5O_{12}$ single crystals irradiated with $^{84}Kr^{+}$ ions, *Physica Status Solidi (b)*, 2022, **259**, 2100415, doi: 10.1002/pssb.202100415.
[42] V. Pankratova, V. A. Skuratov, O. A. Buzanov, A. A. Mololkin, A. P. Kozlova, A. Kotlov, A. I. Popov, V. Pankratov, Radiation effects in $Gd_3(Al, Ga)_5$: O12: Ce^{3+} single crystals induced by swift heavy ions, *Optical Materials: X*, 2022, **16**, 100217, doi: 10.1016/j.omx.2022.100217.
[43] R. Devanathan, Radiation damage evolution in ceramics, *Nuclear Instruments and Methods in Physics Research Section B: Beam Interactions with Materials and Atoms*, 2009, **267**, 3017-3021, doi: 10.1016/j.nimb.2009.06.020.
[44] V. I. Dubinko, A. A. Turkin, D. I. Vainshtein, H. W. den Hartog, New mechanism for radiation defect production and aggregation in crystalline ceramics, *Journal of Nuclear Materials*, 2001, **289**, 86-95, doi: 10.1016/s0022-3115(00)00686-3.
[45] A. E. Kurakhmedov, A. K. Morzabayev, V. V. Uglov, A. L. Kozlovskiy, Study of the effect of variation in the phase composition of ZrO_2/MgO ceramics on the resistance to radiation damage during irradiation with Kr^{15+} ions, *Journal of Composites Science*, 2023, **7**, 497, doi: 10.3390/jcs7120497.

[46] K. Sickafus, E. Montaner, Fundamental studies of radiation damage in two-phase oxide composites, Los Alamos National Lab.(LANL), Los Alamos, NM (United States), 2000.
[47] H. Wang, J. Qi, H. Guo, R. Chen, M. Yang, Y. Gong, Z. Huang, Q. Shi, W. Liu, H. Wang, T. Lu, Influence of helium ion radiation on the nano-grained Li_2TiO_3 ceramic for tritium breeding, *Ceramics International*, 2021, **47**, 28357-28366, doi: 10.1016/j.ceramint.2021.06.253.
[48] Y. Al-Khatatbeh, K. K. M. Lee, B. Kiefer, Phase relations and hardness trends of ZrO_2 phases at high pressure, *Physical Review B*, 2010, **81**, 214102, doi: 10.1103/physrevb.81.214102.
[49] V. V. Bulatov, L. L. Hsiung, M. Tang, A. Arsenlis, M. C. Bartelt, W. Cai, J. N. Florando, M. Hiratani, M. Rhee, G. Hommes, T. G. Pierce, T. D. de la Rubia, Dislocation multi-junctions and strain hardening, *Nature*, 2006, **440**, 1174-1178, doi: 10.1038/nature04658.
[50] M. Ramachandra, A. Abhishek, P. Siddeshwar, V. Bharathi, Hardness and wear resistance of ZrO_2 nano particle reinforced Al nanocomposites produced by powder metallurgy, *Procedia Materials Science*, 2015, **10**, 212-219, doi: 10.1016/j.mspro.2015.06.043.
[51] F. Hou, W. Wang, H. Guo, Effect of the dispersibility of ZrO_2 nanoparticles in Ni–ZrO_2 electroplated nanocomposite coatings on the mechanical properties of nanocomposite coatings, *Applied Surface Science*, 2006, **252**, 3812-3817, doi: 10.1016/j.apsusc.2005.05.076.
[52] S. A. Ghyngazov, V. A. Boltueva, J. H. O'Connell, T. N. Vershinina, N. S. Kirilkin, R. A. Rymzhanov, V. A. Skuratov, A. P. Surzhikov, Swift heavy ion induced phase transformations in partially stabilized ZrO_2, *Radiation Physics and Chemistry*, 2022, **192**, 109917, doi: 10.1016/j.radphyschem.2021.109917.
[53] M. Alin, A. L. Kozlovskiy, M. V. Zdorovets, V. V. Uglov, Study of the mechanisms of the t-ZrO_2 → c-ZrO_2 type polymorphic transformations in ceramics as a result of irradiation with heavy Xe^{22+} ions, *Solid State Sciences*, 2022, **123**, 106791, doi: 10.1016/j.solidstatesciences.2021.106791.
[54] K. E. Sickafus, H. Matzke, T. Hartmann, K. Yasuda, J. A. Valdez, P. Chodak, M. Nastasi, R. A. Verrall, Radiation damage effects in zirconia, *Journal of Nuclear Materials*, 1999, **274**, 66-77, doi: 10.1016/s0022-3115(99)00041-0.
[55] G. W. Egeland, J. A. Valdez, S. A. Maloy, K. J. McClellan, K. E. Sickafus, G. M. Bond, Heavy-ion irradiation defect accumulation in ZrN characterized by TEM, GIXRD, nanoindentation, and helium desorption, *Journal of Nuclear Materials*, 2013, **435**, 77-87, doi: 10.1016/j.jnucmat.2012.12.025.
[56] A. L. Kozlovskiy, M. V. Zdorovets, Study of the radiation disordering mechanisms of AlN ceramic structure as a result of helium swelling, *Journal of Materials Science: Materials in Electronics*, 2021, **32**, 21658-21669, doi: 10.1007/s10854-021-06684-x.
[57] V. V. Bulatov, L. L. Hsiung, M. Tang, A. Arsenlis, M. C. Bartelt, W. Cai, J. N. Florando, M. Hiratani, M. Rhee, G. Hommes, T. G. Pierce, T. D. de la Rubia, Dislocation multi-junctions and strain hardening, *Nature*, 2006, **440**, 1174-1178, doi: 10.1038/nature04658.
[58] Q. Xie, Z. Li, H. Ma, S. Liu, X. Liu, J. Liu, J. J. Sidor, Correlation between dislocation hardening and the geometrically-necessary-dislocation densities in a hexagonal-close-packed Zr-2wt%Ti alloy, *Materials Science and Engineering: A*, 2023, **868**, 144768, doi: 10.1016/j.msea.2023.144768.

Publisher's Note: Engineered Science Publisher remains neutral with regard to jurisdictional claims in published maps and institutional affiliations.

